

UNCLASSIFIED

Defense Technical Information Center
Compilation Part Notice

ADP013363

TITLE: The Dependence of Dielectric Properties on Composition Variation in Ba_{0.6}Sr_{0.4}[YTa]_yTi_{1-2y}O₃

DISTRIBUTION: Approved for public release, distribution unlimited

This paper is part of the following report:

TITLE: Materials Research Society Symposium Proceedings; Volume 720. Materials Issues for Tunable RF and Microwave Devices III Held in San Francisco, California on April 2-3, 2002

To order the complete compilation report, use: ADA410712

The component part is provided here to allow users access to individually authored sections of proceedings, annals, symposia, etc. However, the component should be considered within the context of the overall compilation report and not as a stand-alone technical report.

The following component part numbers comprise the compilation report:

ADP013342 thru ADP013370

UNCLASSIFIED

The Dependence of Dielectric Properties on Composition Variation in



Daniel Potrepka, Steven Tidrow, Arthur Tauber, Kevin Kirchner, Matthew Ervin, Krishna Deb, Bernard Rod, and Frank Crowne

Sensors & Electron Devices Directorate, U.S. Army Research Laboratory, Adelphi, MD 20783-1197, U.S.A.

ABSTRACT

$\text{Ba}_{0.6}\text{Sr}_{0.4}(\text{YTa})_y\text{Ti}_{1-2y}\text{O}_3$ has been shown to have properties which are promising for tunable applications requiring low dielectric constant [1]. $\text{Ba}_{0.6}\text{Sr}_{0.4}(\text{YTa})_y\text{Ti}_{1-2y}\text{O}_3$ with $y \leq 0.10$ has been synthesized and well-characterized using x-ray diffraction, EDAX, and Raman Spectroscopy. The dependence of the dielectric properties on concentration, y , of Y and Ta are discussed along with implications for improved performance in device applications.

INTRODUCTION

It has been shown that binary charge-balanced substitutions of 3+ and 5+ ions into the B site (for Ti^{4+}) in $\text{Ba}_{1-x}\text{Sr}_x\text{TiO}_3$ (BST) lead to changes in the characteristics of the ferroelectric (FE) transition, Curie Temperature (T_c), and tunability of the dielectric constant that do not occur for non-charge-compensated doping of BST or for 4+ substitutions into the Ti^{4+} site [1,2]. The binary charge-balanced substitution of 3+ and 5+ ions for Ti lead to greater applicability of the FE technology due to broader temperature ranges of operation which include the U. S. Military Specification temperature range (mil spec). Such behavior is consistent with device requirements as discussed in References [3,4] where tunability is of major importance but losses are of less importance. For certain choices of charge-balanced substitution of 3+ and 5+ ions, T_c shifts dramatically by as much as -60°C or more accompanied by a significant broadening of the FE transition. The behavior of the tunability in such cases is similar to that of the dielectric constant, reflecting the broadening and shifting of the difference between the dielectric constant at zero electric field and the dielectric constant tuned by the application of a DC electric field. This paper focuses on research investigations which seek to characterize, in more detail, the compositional dependence of the dielectric properties due to simultaneous variation of the Y and Ta content in the Ti site. Results of effects of sintering temperature (T_s) on selected charge-balanced substitutions, y , are presented and discussed. The character of the synthesized material has been studied using x-ray diffraction, Raman spectroscopy, density, and SEM measurements. Electrical properties were obtained through studies of the temperature dependence of the capacitance. The lattice constant, grain size, dielectric constant, tunability, and an electric-field- and temperature-dependent figure of merit (FOM) were studied to determine the effects of the Y and Ta concentration variation and changes in T_s .

EXPERIMENTAL DETAILS

Compositions of $\text{Ba}_{0.6}\text{Sr}_{0.4}(\text{YTa})_y\text{Ti}_{1-2y}\text{O}_3$ with $y \leq 0.10$ were prepared by mixing BaCO_3 , SrCO_3 , Y_2O_3 , Ta_2O_5 , and TiO_2 in stoichiometric proportions. The samples were then ground and pressed into pellets which were calcined at 1100°C for 8 hours. Next the samples were reground

and pressed at 50 kpsi, then sintered between 1450 °C and 1600 °C. There were particular samples with $y = 0.03$ and 0.05 , which were separated into two parts of equal mass prior to sintering. One portion of each composition was then sintered at a temperature of $T_s = 1550$ °C and the other was sintered at 1600 °C. After sintering, a portion of each synthesized sample was cut away and ground and polished. Volume densities were obtained on a microbalance, θ - 2θ x-ray diffraction scans and diffraction ring graphs were obtained using Cu K α 1 radiation, and Raman spectroscopy was performed. For each sample, contacts were then deposited to form a parallel plate capacitor, and capacitance was measured at a sampling frequency of 1 MHz with applied DC electric fields in the range $0 \leq E \leq 1$ V/ μ m and the temperature varied over -75 °C $\leq T \leq 100$ °C using an environmental chamber. Selected samples were fractured and the grain structure was studied using SEM. Nominal grain sizes were estimated for samples with different y .

RESULTS

The ratio of the volume density to the theoretical value (in percent) was found to drop from ~ 95 % for $y = 0$ to ~ 60 % for $y \geq 0.03$. Theoretical densities were estimated using the lattice constants obtained by x-ray diffraction measurements. For samples with $y = 0.03$ and 0.05 that were sintered at 1450 – 1600 °C, T_s was found to have a modest effect on density, with the density increasing up to 10% with increases over this temperature range. The x-ray diffraction scans show that the samples are single phase and cubic up to $y = 0.08$. At $y = 0.10$ a peak due to second phase appears at $d = 3.06502$ Å and splitting is observed in the major peaks that are significantly above the noise levels indicating deviation from the cubic structure. For $y = 0.05$, spots associated with the beginnings of grain size enhancement or grain growth ordering in the samples were more enhanced in the x-ray diffraction rings for samples sintered at 1600 °C than at 1550 °C. Spots indicative of grain growth were seen in the rings for the $y = 0.03$ sample sintered at 1550 °C. In addition, for $T_s = 1600$ °C compared to $T_s = 1450$ °C, the lattice constant is smaller by a significant amount (0.005 Å) for $y = 0.03$, but by an insignificant amount (≤ 0.003 Å) for $y = 0.05$. This may be an indication of ordering [5]. There was no evidence of superlattice peaks in the x-ray diffraction scans. Further evidence of the nature of the lattice was obtained from the Raman studies. For $y \leq 0.05$, the 306 cm^{-1} position associated with the E(TO₂) Raman line in BaTiO₃ was monitored. The absence of an E(TO₂) peak was observed on a linear scale. This is consistent with the expected behavior for Ba_{1-x}Sr_xTiO₃, $x \geq 0.32$ [6]. However, on a log scale, there appears a shallow bump at ~ 306 cm^{-1} for each sample in the range $0.01 \leq y \leq 0.05$ (Figure 1) which may be evidence of the onset, with YTa concentration, of the noncubic phase observed in the θ - 2θ diffraction scan for the $y = 0.10$ phase.

Nominal grain sizes estimated from the SEM studies of samples are shown in Figure 2 for T_s and y values. The grain size drops by an order of magnitude from ~ 30 μ m for $y = 0$ (BST) to ~ 1 μ m for $y = 0.01$. Grain-like features are observed for $0.04 \leq y \leq 0.10$ at low T_s (1450 °C – 1500 °C) but do not appear to be well-defined. In all samples with $y > 0$, the porosity of the samples due to Ostwald ripening [7] can be observed and volume densities are ~ 65 % compared to ~ 93 % for $y = 0$. For $y = 0.03$ and 0.05 , at the more elevated T_s values of 1550 °C and 1600 °C, distinct cubic grain features are clearly seen in the cleaved sections and at the walls of the porous regions. For an increase in T_s from 1550 °C to 1600 °C, the grain size is estimated to double, from 1 μ m to 2 μ m for both the $y = 0.03$ and the $y = 0.05$ samples.

The dielectric constant (real relative permittivity, ϵ) plotted versus temperature (Figure 3) is consistent with similar plots for the general case of simultaneous substitution of 3+ and 5+

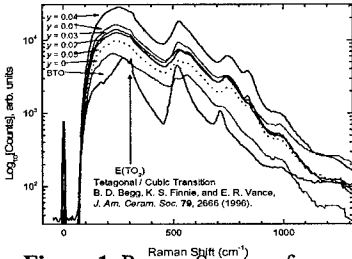


Figure 1. Raman Spectra of $Ba_{0.6}Sr_{0.4}(YTa)_yTi_{1-2y}O_3$

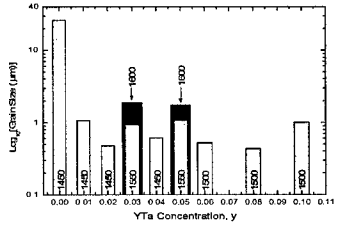


Figure 2. Grain Size vs YTa content, y . Numbers denote sinter temperature, T_s ($^{\circ}C$).

ions for Ti as reported in References [1,2]. In that work, T_c shifted to lower temperature, the FE transition broadened and the magnitude of ϵ was markedly reduced for small concentrations ($y = 0.03$) for many such ion pairs. In comparison, substitutions of 4+ ions for Ti do not shift the T_c of BST very much but can broaden the FE transition and reduce ϵ [2,8]. The behavior of T_c with concentration of Y and Ta is plotted in Figure 4 (in analogy to similar plots for BST [8]) and that of the peak value of the dielectric constant $\epsilon(T_c)$, in Figure 5. For Figure 5, the values of $\epsilon(T_c)$ for $y = 0.08$ and 0.10 are obtained by a graphical extrapolation of Fig. 4 and of $\epsilon(T)$ below the minimum measurement temperature, $-75^{\circ}C$, of the environmental chamber. For the device applications that these studies are relevant to, temperature-insensitive materials over the mil spec range are desired so that the device can operate without the added burden of refrigeration or heating and to eliminate sensitivity to sudden temperature spikes or fluctuations. The material must also be highly-tunable [4]. Therefore, a figure of merit (FOM) was developed for the perovskites studied which is given by the expression,

$$FOM = \frac{(\Delta\epsilon / \Delta E)}{(\Delta\epsilon / \Delta T)} \quad (1)$$

Figure 6 shows the tunability plots for $y \leq 0.10$ and their respective values of the FOM evaluated

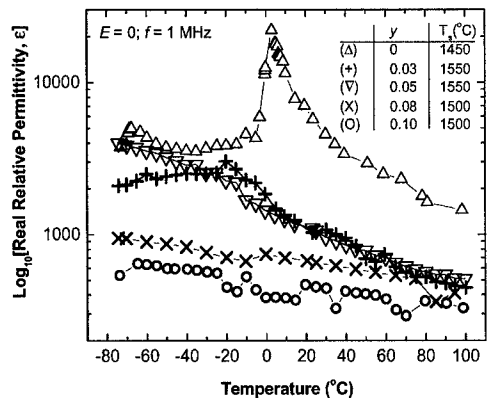


Figure 3. Dielectric constant vs temperature for $y \leq 0.10$, $T_s \leq 1550^{\circ}C$.

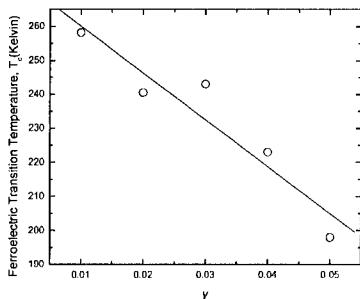


Figure 4. Ferroelectric Transition Temperature, T_c , vs YTa content, y .

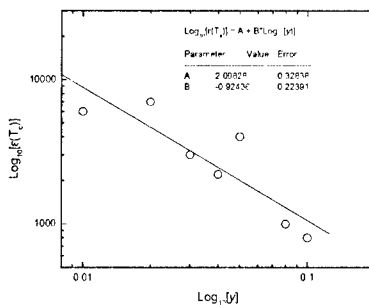


Figure 5. Dielectric constant at the critical temperature, $\epsilon(T_c)$, vs YTa content, y .

at the maximum dielectric constant measured. This FOM is largest at the intermediate concentration of $y = 0.05$. More importantly, the FE transition and tunability broaden as y increases, and the FOM approaches a constant value over a larger portion of the mil spec range.

Figure 7 shows ϵ plotted versus temperature for $y = 0.03$ and 0.05 and $T_s = 1550^\circ\text{C}$ and 1600°C . Figure 8 shows the corresponding tunability plots and their FOM values. Recall that, in Figure 2, increased concentrations, y , of Y and Ta reduce the grain size for low T_s ($\leq 1550^\circ\text{C}$), but this can be reversed somewhat with increase in T_s with very little measured change in density. Spots, which are an indication of grain growth, begin to occur in the area detector images obtained from x-ray diffraction at 1550°C and 1600°C . Also for increase in T_s from 1550°C to 1600°C , grain size increases and grains become more faceted, as observed in the SEM micrographs, plus the FE transition is sharpened. Since grain size increases were observed for both decreased y and increased T_s , one may thus wish to see if grain size changes are the sole cause of the changes in the ferroelectric nature of the BST as Y and Ta are added while maintaining charge balance. However, when grain size is increased due to increase in T_s , not all the electrical characteristics are reversed relative to those due to decrease in y . T_c shifts to a lower temperature with both increased y and increased T_s . So the changes in the grain size that occur for changes in y due to increased but charge-balanced additions of Y and Ta to BST do not appear to be the sole cause of changes in the nature of the ferroelectric transition away from that of BST as y increases. A study of the dielectric constant and tunability for the $y = 0.03$ sample in

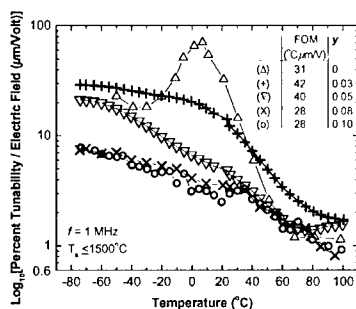


Figure 6. Percent tunability / Electric Field and figure of merit for $y \leq 0.10$.

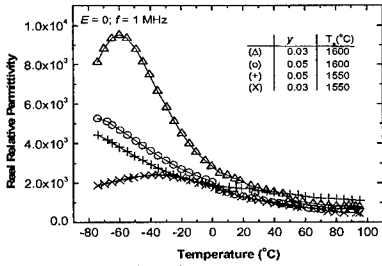


Figure 7. Dielectric constant vs temperature for $T_s = 1550$ °C, 1600 °C.

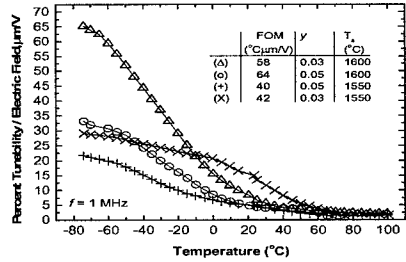


Figure 8. Percent tunability / E-Field and figure of merit (FOM), inset.

Figures 7 and 8 further shows that $\epsilon(T)$ at the higher $T_s = 1600$ °C, relative to that at the lower $T_s = 1550$ °C, is sharper and higher in magnitude at or near the perceived T_c as though returning to a state more like that of BST, except shifted to a lower T_c . The $y = 0.05$ sample appears to have the same trend, although T_c is below the range of measurement. The FOM although lower by about 30 % for the $T_s = 1550$ °C samples applies over a broader temperature range than the FOM for $T_s = 1600$ °C. Room-temperature losses at 1 kHz for the various y and T_s are given in Table I. It of note that for the samples with $T_s = 1600$ °C, even though the measurements are made well above T_c , in the paraelectric (PE) regime, the losses are larger, by a factor of ten, than those for samples sintered at 1550 °C. This implies a resistance of FE domains to respond to external fields in the samples sintered at $T_s = 1600$ °C compared to those sintered at 1550 °C.

The shift in the T_c as a result of the introduction of $Y^{3+}Ta^{5+}$ pairs in the B site of BST (which does not occur for 4+ ion substitutions) suggests an array of dipole pairs distributed throughout the PE/FE domains in which the FE long range order is modified in such a way that T_c is shifted to a lower temperature compared to the unsubstituted BST. This modification occurs in coincidence with a reduction of grain size that correlates with the broadening of the FE transition. The sharpening of the FE transition, observed for $y = 0.03$ when T_s is increased from 1550 °C to 1600 °C, also correlates with increase in grain size. The fact that T_c shifts to a lower temperature and losses increase at room temperature (well above T_c), at $y = 0.03$ for T_s increased from 1550 °C to 1600 °C, suggests a difference in the nature of the relationship between the $Y^{3+}Ta^{5+}$ pairs and the FE/PE environments in these two samples. More studies are needed. Theoretical studies of how T_c is affected by the competition between short range dipole forces and the long range order of ferroelectricity in a dense frozen dipolar system have been carried

Table I			
Dissipation Factor, D, and Quality Factor, Q, at 1 kHz			
y	T_s (°C)	D	Q
0	1450	0.005	200
0.02	1450	0.008	125
0.03	1450	0.002	500
0.04	1450	0.003	333
0.05	1500	0.005	200
0.06	1500	0.003	333
0.08	1500	0.005	200
0.10	1500	0.002	500
0.03	1550	0.003	333
0.05	1550	0.003	333
0.03	1600	0.03	33
0.05	1600	0.02	50

out by Klapp and Patey [9]. A number of other papers discuss dipolar effects in ferroelectrics (see for example References [10-13]) and the shift in $\epsilon(T_c)$ of Fig. 5 is modeled in [13], but there is no theoretical discussion of small percentages of 3+ and 5+ ions in charge-balanced substitution for the majority 4+ ions (which in our case is Ti^{4+}) in the B site of perovskites, which predict the observed T_c shifts.

CONCLUSIONS

Tunability, characterized by FOM, is the key parameter in frequency-agile device studies at ARL [4]. A study has been made to better understand the effects of concentration, y , and sinter temperature, T_s , on tunability in charge-balanced, 3+ and 5+ substitutions for Ti in BST. For $T_s \leq 1550$ °C, increases in y cause T_c to decrease and the FE transition to broaden, leading to a reduction and less variation in dielectric constant, improvement in FOM over the mil spec range as $\epsilon(T)$ and tunability broaden, and decrease in grain size. An increase in T_s , from 1550 °C to 1600 °C, also causes T_c to decrease. However, the FE transition sharpens, $\epsilon(T_c)$ increases, tunability increases near T_c (but FOM decreases away from T_c), grain size increases, and Q is reduced. For device applications, the improved FOM over the mil spec range, due to charge-balanced substitutions with $T_s \leq 1550$ °C, small grain size, and broad FE transition, is preferred.

ACKNOWLEDGEMENTS

DMP acknowledges the National Research Council for their support during his tenure, completed in Dec 2001, as a Postdoctoral Associate.

REFERENCES

1. D. M. Potrepka, S. C. Tidrow, and A. Tauber, *Mat. Res. Soc. Symp. Proc.* **656E**, DD5.9.1 (2001).
2. D. M. Potrepka, S. C. Tidrow, and A. Tauber, to be published in *Integrated Ferroelectrics* **42**, 97 (2002).
3. S. C. Tidrow *et al.*, *Integrated Ferroelectrics* **28**, 151 (2000).
4. F. J. Crowne and S. C. Tidrow in *Materials Issues for Tunable RF and Microwave Devices III, Proceedings of 2002 MRS Spring Meeting*, paper number H6.5, San Francisco, CA (2002).
5. P. Woodward, R.-D. Hoffmann, and A.W. Sleight, *J. Mater. Res.* **9**, 2118 (1994).
6. P. S. Dobal *et al.*, *Journal of Raman Spectroscopy* **32**, 147 (2001); B. D. Begg, K. S. Finnie, and E. R. Vance, *J. Am. Ceram. Soc.* **79**, 2666 (1996).
7. D. Kolar, *Proceedings of the International Conference on the Chemistry of Electronic Ceramic Materials*, edited by Peter K. Davies and Robert S. Roth, (NIST, 1990), p.3.
8. F. S. Galasso, *Perovskites and High T_c Superconductors*, Gordon and Breach (1990), p. 108.
9. S. H. L. Klapp and G. N. Patey, *J. Chem. Phys.* **115**, 4718 (2001).
10. B. E. Vugmeister and M. D. Glinchuk, *Rev. Mod. Phys.* **62**, 993 (1990).
11. S. M. Emyanov *et al.*, *Phase Transitions* **A45**, 251 (1993).
12. B. Dkhil *et al.*, *Phys. Rev. B* **65**, 024104/1 (2002).
13. F. J. Crowne *et al.* in *Materials Issues for Tunable RF and Microwave Devices III, Proceedings of 2002 MRS Spring Meeting*, paper number H5.1, San Francisco, CA (2002).